

# Low-field low-temperature magnetotransport studies of CeP

T. Terashima

*Tsukuba Magnet Laboratory, National Research Institute for Metals, 3-13 Sakura, Tsukuba, Ibaraki 305-0003, Japan*

J. S. Qualls, T. F. Stalcup, and J. S. Brooks

*National High Magnetic Field Laboratory, Tallahassee, Florida 32310*

H. Aoki

*Center for Low Temperature Science, Tohoku University, Sendai, Miyagi 980-8578, Japan*

Y. Haga

*Japan Atomic Energy Research Institute, Tokai, Ibaraki 319-1195, Japan*

A. Uesawa and T. Suzuki

*Department of Physics, Tohoku University, Sendai, Miyagi 980-8578, Japan*

(Received 29 March 1999; revised manuscript received 9 September 1999)

Magnetoresistance measurements on CeP have been performed between about 5 and 40 K in magnetic fields up to 6 T. A complex phase diagram with six different phase transitions is derived. In particular, we find a second phase transition in the supposed antiferromagnetic phase at zero-magnetic field. The magnetotransport behavior is discussed in relation to the magnetic structure in each phase. [S0163-1829(99)05245-5]

## I. INTRODUCTION

CeP is a cubic compound with the NaCl structure. It is a compensated semimetal with electrons and holes originating mainly from the Ce 5*d* and P 3*p* states, respectively. The carrier density is very low, estimated from Hall measurements to be about 1%/Ce or less.<sup>1</sup> The compound has been an object of extensive studies these years because of various intriguing phenomena.<sup>2</sup> The electrical resistivity  $\rho$  shows a negative temperature derivative down to about 80 K,<sup>3</sup> which is a great contrast to a simple metallic behavior found in the diluted compound  $\text{Ce}_x\text{La}_{1-x}\text{P}$  ( $x=0.02$ ).<sup>4</sup> Further, the resistivity of CeP at 80 K is one order-of-magnitude larger than that of the diluted compound.<sup>4</sup> Magnetic properties are still more mysterious; long-period magnetic structures with unexpected large-moment states (Ref. 5) as well as successive metamagnetic transitions (Refs. 6 and 7) are notable among others. It is generally assumed that a strong interplay between the sparse carriers and the Ce 4*f* localized magnetic moments underlies these anomalies.

Figure 1 shows the magnetic phase diagram determined in the present study. The crystal-field ground state of the  $\text{Ce}^{3+}$  ion in the paramagnetic phase is  $\Gamma_7$  with  $\Gamma_8$  sitting at about 160 K above.<sup>8</sup> In a magnetic field of about 2 T or higher parallel to [001], CeP shows two distinct magnetic phase transitions, denoted by  $F(\Gamma_8)$  and  $AF(\Gamma_7)$  in the figure, with decreasing temperature.<sup>3</sup> The former transition  $F(\Gamma_8)$  is characterized by the appearance of a ferromagnetic moment. The magnetic structure in phase III has been determined from neutron diffraction experiments to be regular stacking of two ferromagnetic and eight paramagnetic (001) layers.<sup>5</sup> The Ce ions in the ferromagnetic double layers have the magnetic moment of  $2 \mu\text{B}/\text{Ce}$ . Since the large moment is not compatible with the  $\Gamma_7$  ground state in the paramagnetic

phase, those Ce ions were assumed to be in the  $\Gamma_8$  state. Recent magnetic form factor measurements with polarized neutrons have confirmed this view; i.e., the form factor determined for those Ce ions is very close to that expected for the crystal-field  $\Gamma_8$  state.<sup>9</sup> The ferromagnetic  $\Gamma_8$  double layers being intact, a type-I-like antiferromagnetic order develops among the remaining paramagnetic ions below the transition  $AF(\Gamma_7)$ .<sup>5</sup> The Ce ions in the antiferromagnetic part have a  $\Gamma_7$ -compatible moment of  $0.7 \mu\text{B}/\text{Ce}$  and constitute a

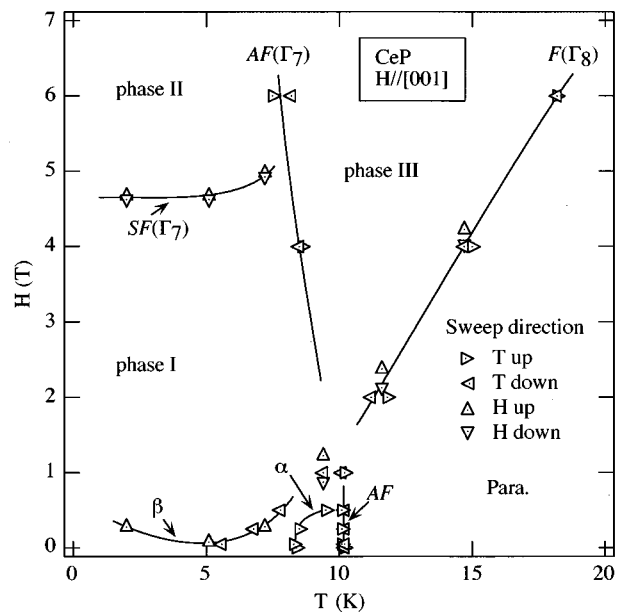


FIG. 1. Magnetic phase diagram of CeP determined from resistivity measurements in this study. The phase boundaries,  $\alpha$ ,  $\beta$ ,  $AF$ ,  $F(\Gamma_8)$ ,  $AF(\Gamma_7)$ , and  $SF(\Gamma_7)$ , are shown; see text for their description.

ferromagnetic (001) layer, which couples antiferromagnetically along the [001] axis. The total composite magnetic structure is an eleven-layer one composed of ferromagnetic  $\Gamma_8$  double layers and antiferromagnetically coupled nine  $\Gamma_7$  layers. The direction of the  $\Gamma_7$  moment is parallel and perpendicular to the applied field in the phases I and II, respectively, and hence the transition  $SF(\Gamma_7)$  may be regarded as a spin-flop transition in the antiferromagnetic  $\Gamma_7$  order.

Magnetic ordering at lower fields ( $H < \sim 2$  T), especially at zero field, is less obvious. Previous low-field magnetization studies found two phase transitions.<sup>10</sup> One is an antiferromagnetic transition at the Néel temperature  $T_N$  of 10 K (the transition  $AF$  in Fig. 1), whereas the other at a lower temperature is accompanied by a ferromagnetic moment and was attributed to a transition to the phase I (our  $\beta$  transition probably corresponds to this, see Fig. 1). As the latter transition was not observed at zero field, it was concluded that CeP is a simple antiferromagnet at zero field. The conclusion was reinforced by the observation that the neutron diffraction pattern at zero field at 5 K was found to be compatible with the type-I antiferromagnetic structure.<sup>5</sup> However, there are pieces of evidence suggesting that a second transition occurs below  $T_N$  even without applied fields. In specific heat measurements, for example, a shoulder was observed at around 8 K in addition to a sharp peak at  $T_N$  of 10.2 K.<sup>3,10</sup>

In this paper, we identify six different magnetic phase transitions through detailed magnetoresistance measurements and provide a complete low-field description of the phase diagram. In particular, by finding the two phase transitions  $AF$  and  $\alpha$  at zero field (see Fig. 1), we clarify that CeP is not a simple type-I antiferromagnet even without applied fields. We will argue that the  $\alpha$  transition is ascribable to appearance of  $\Gamma_8$  layers. Further, peculiar magnetotransport properties in CeP will be discussed with emphasis on roles played by  $\Gamma_8$  layers.

## II. EXPERIMENTAL PROCEDURES AND RESULTS

The single crystal used in this study was grown by a recrystallization method.<sup>3</sup> The resistivity was measured as a function of the temperature  $T$  ( $\sim 5$  K  $< T < 40$  K) and also as a function of the magnetic field  $H$  applied along [001] ( $H < \sim 6$  T), using a standard four contact method with a low-frequency ac current ( $f = 72$  Hz). By using a rotating sample holder, we could switch between the longitudinal ( $I \parallel H, \rho_l$ ) and transverse ( $I \perp H, \rho_t$ ) configurations *in situ*. Since CeP is known to exhibit a strong hysteresis effect,<sup>11</sup> the following procedures were followed to obtain reproducible results. Before starting a temperature or field cycle for data acquisition, the sample was always heated above 30 K ( $\gg T_N$ ) and cooled in zero-magnetic field down to the lowest temperature or a target temperature. For  $\rho$  vs  $T$  measurements, the magnetic field was applied at the lowest temperature, and then up- and down-sweep data were consecutively taken in that order.

The  $\rho$  vs  $T$  curve at zero field is shown in Fig. 2(a) together with the temperature derivative  $d\rho/dT$  (also see Fig. 3 for a wider temperature range). The peak at about 10 K signals the antiferromagnetic transition. Defining  $T_N$  as the temperature where  $d\rho/dT$  shows a maximum, we obtain  $T_N = 10.2$  K, which is in good agreement with previously re-

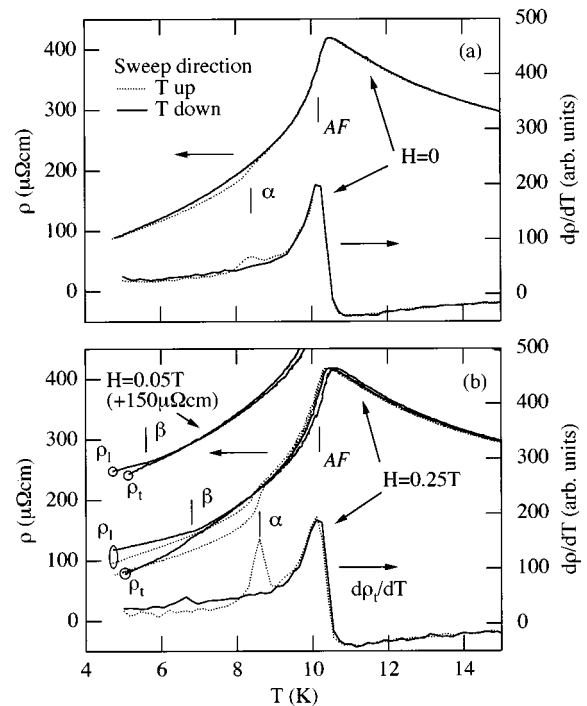


FIG. 2. Resistivity and its temperature derivative for (a)  $H = 0$ , and (b)  $H = 0.05$  and  $0.25$  T. The  $H = 0.05$  T curve is shifted by  $150 \mu\Omega \text{ cm}$ .  $\rho_l$  and  $\rho_t$  denote longitudinal and transverse resistivities, respectively. The phase transitions  $\alpha$ ,  $\beta$ , and  $AF$  are marked.

ported values.<sup>3,10,12</sup> We notice that hysteresis is absent at  $T_N$  and that it arises only at temperatures well below  $T_N$ . Similar behavior was noted in previous thermal expansion measurements.<sup>12</sup> The absence of hysteresis at  $T_N$  is consistent with a usual antiferromagnetic transition, which is of second order, while the hysteresis at lower temperatures suggests existence of another transition. A small cusp appears at 8.4 K in the  $d\rho/dT$  trace for the increasing- $T$  sweep (dotted line) and confirms the second transition  $\alpha$ , responsible for the hysteresis, even though the transition temperature is not discernible in the decreasing- $T$  sweep.

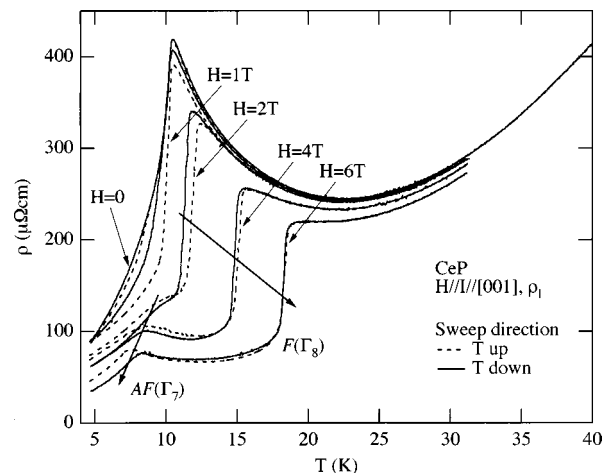


FIG. 3. Resistivity as a function of the temperature at zero field and at longitudinal fields up to 6 T. The magnetic field dependence of the phase transitions  $F(\Gamma_8)$  and  $AF(\Gamma_7)$  are indicated by arrows.

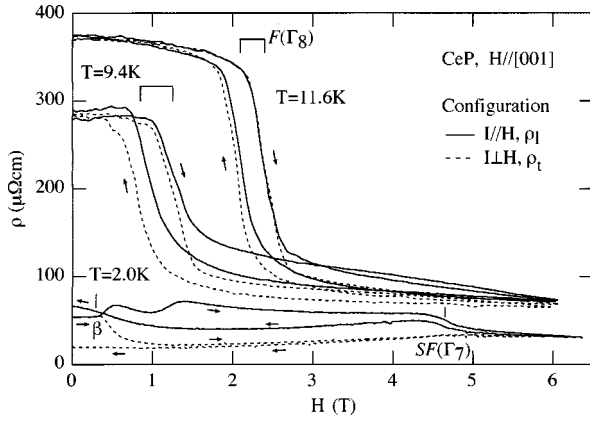


FIG. 4. Resistivity as a function of the magnetic field. Arrows indicate directions of field sweeps. The phase transitions  $\beta$ ,  $SF(\Gamma_7)$ , and  $F(\Gamma_8)$  are marked.

The  $\rho_i$  vs  $T$  ( $i=l$  and  $t$ ) and  $d\rho_i/dT$  vs  $T$  traces at 0.25 T are shown in Fig. 2(b). Given our temperature accuracy of about 1%,  $T_N$  is the same as the zero-field value and no hysteresis is appreciable at  $T_N$ . The  $\alpha$  transition is clearly observed at 8.5 K in the increasing- $T$  traces (dotted lines). Comparing  $\rho_l$  and  $\rho_t$  for decreasing- $T$  sweeps (solid lines), we find an anomaly; i.e., the difference between  $\rho_l$  and  $\rho_t$  starts to grow rapidly below about 7 K. We attribute this anomaly  $\beta$  to a phase transition, although it is not necessarily a counterpart of the  $\alpha$  transition since the hysteresis loop does not close. The anomaly  $\beta$  is found to exist even at 0.05 T (shifted curves).

The  $\rho_l$  vs  $T$  curves at 1 T and higher are shown in Fig. 3. The  $H=1$  T trace shows a cusp at almost the same temperature as the zero-field trace. The character of the transition, however, differs from the antiferromagnetic transition at lower fields; i.e., significant hysteresis starts from above the transition temperature. For magnetic fields higher than 1 T, the data are readily interpreted. The large sharp resistivity drops accompanied by hysteresis are attributed to the transition  $F(\Gamma_8)$ , whereas broad maxima at lower temperatures are due to the transition  $AF(\Gamma_7)$ . The magnetoresistance ratio,  $[\rho(0) - \rho(H)]/\rho(0)$ , amounts to 0.83 at 6 T near 10 K.

Figure 4 shows  $\rho_l$  and  $\rho_t$  at 2.0, 9.4, and 11.6 K as a function of  $H$ . The resistivity at 2.0 K is almost constant until about 0.3 T where  $\rho_l$  and  $\rho_t$  separate. The longitudinal resistivity  $\rho_l$  starts to increase while  $\rho_t$  decreases. This behavior is reminiscent of the  $\beta$  anomaly observed in the  $\rho$  vs  $T$  curves at low fields. Indeed, the  $\beta$  anomalies determined from the  $\rho$  vs  $H$  and  $\rho$  vs  $T$  traces lie on a single curve in a  $H$ - $T$  phase diagram (Fig. 1). The resistivity in a field regime just above the  $\beta$  anomaly shows a sample-dependent behavior; for the present sample,  $\rho_l$  exhibits two broad peaks above the  $\beta$  anomaly whereas we observed only one peak in our previous measurements on a different sample.<sup>7</sup> The drop in  $\rho_t$  at 4.7 T is due to the transition  $SF(\Gamma_7)$ , where  $\rho_t$  shows a slight bend. For the decreasing- $H$  sweeps, no sign of the  $\beta$  anomaly is found. Hysteresis loops do not close and a noticeable difference between  $\rho_l$  and  $\rho_t$  remains at zero field. Similar zero-field anisotropy also appears at 5.1 and 7.2 K after application of fields (data not shown). The resistivity at 9.4 K shows a large decrease with significant hysteresis at about 1 T. This transition links the  $\beta$  and  $F(\Gamma_8)$  lines in the

phase diagram (Fig. 1). We note that  $\rho_l$  and  $\rho_t$  coincide at zero field after removal of the field. The resistivity drop with hysteresis at about 2 T in the  $T=11.6$  K traces is due to the transition  $F(\Gamma_8)$ .

The  $H$ - $T$  phase diagram thus determined is shown in Fig. 1 and is in general agreement with those previously reported.<sup>3,5-7,10</sup>

### III. DISCUSSION

The observation of the  $\alpha$  transition at zero field clearly indicates that the type-I antiferromagnetic phase is stable only in a narrow temperature region below  $T_N$  and that a second low-temperature phase exists at lower temperatures. The absence of a clear transition in decreasing- $T$  sweeps suggests that the lowest-temperature phase develops very gradually with decreasing temperature, and/or substantial disorder in the magnetic structure.

We ascribe the lowest-temperature phase to appearance of  $\Gamma_8$  layers. Existence of  $\Gamma_8$  layers does not contradict the reported zero-field neutron diffraction pattern as long as the  $\Gamma_8$  layers randomly replace  $\Gamma_7$  layers with the same moment direction. The staggered moment of  $0.8 \mu_B/\text{Ce}$  estimated from the zero-field pattern is slightly larger than the  $\Gamma_7$  moment ( $0.714 \mu_B/\text{Ce}$ ) and it was previously suggested that the excess moment could be attributed to such replacement of  $\Gamma_7$  layers with  $\Gamma_8$  layers.<sup>5</sup> Further, recent magnetostriction (Ref. 12) and thermal expansion measurements (Ref. 13) provide strong evidence for the existence of  $\Gamma_8$  layers in the supposed antiferromagnetic phase at zero field. From direct observation of lattice contraction at the  $F(\Gamma_8)$  transition and also from analysis of the thermal expansion based on the crystal field, the authors of those reports have shown that appearance of  $\Gamma_8$  layers accompanies substantial lattice contraction. Since shrinkage of the lattice is also observed below  $T_N$ , it has been suggested that about 10% of  $\Gamma_7$  layers are replaced with  $\Gamma_8$  layers at zero field below  $T_N$ .

The anomaly  $\beta$  is attributed to a transition from the zero-field low-temperature phase to phase I. In accord with results of previous low-field magnetization measurements,<sup>10</sup> the phase boundary does not intersect the  $T$  axis in the phase diagram (Fig. 1), i.e., the  $\beta$  transition does not occur at zero field.

The appearance of distinct anisotropy between  $\rho_l$  and  $\rho_t$  at the anomaly may be explained as follows. A zero-field-cooled sample is equally divided below  $T_N$  into three types of domains, i.e., the domains in each of which the Ce 4*f* local moment is parallel to [100], [010], or [001]. This domain structure prevents anisotropy, if any, from showing up in the resistivity. As the field is increased along [001], the transition to phase I occurs and the [001] domains grow with increasing magnetic energy gain until the [100] and [010] domains disappear. We note here that the magnetic structure in a [001] domain consists of  $\Gamma_8$  and  $\Gamma_7$  (001) layers and that, for  $\rho_l$  ( $I \parallel [001]$ ,  $H \parallel [001]$ ), the electrical current goes perpendicularly to those layers. Accordingly, we attribute the observed anisotropy ( $\rho_l > \rho_t$ ) to disorder in stacking sequence of the layers. Such stacking faults have been suggested by neutron diffraction experiments (Ref. 5); the correlation length of the eleven-layer magnetic structure was found to be only 50–60 Å and hence it was necessary to

include disorder in the stacking sequence to fit experimental diffraction patterns. The analysis by Kohgi *et al.* indicates that the occupation factor of the  $\Gamma_8$  site in the eleven structure is about 80% and that some  $\Gamma_8$  layers exist randomly replacing  $\Gamma_7$  layers. Those stacking faults, which may be regarded as irregularly instead  $\Gamma_8$  (001) layers, can effectively scatter current carriers moving perpendicular to them.

It is interesting to note that, after application of the field, the anisotropy between  $\rho_l$  and  $\rho_t$  persists to zero field for  $T=2.0, 5.1,$  and  $7.2$  K, but disappears for  $T=9.4$  K (Fig. 4). This difference in behavior supports our interpretation of the  $\alpha$  transition. With decreasing field at  $9.4$  K, we cross the  $\alpha$  phase boundary (Fig. 1), the  $\Gamma_8$  layers melt away, and hence the anisotropy due to the above mechanism vanishes. On the other hand, since we do not cross the  $\alpha$  boundary at the lower temperatures, i.e.,  $2.0, 5.1,$  and  $7.2$  K, the  $\Gamma_8$  layers survive to zero field and hence the anisotropy persists. This conjecture is in line with magnetization data measured at  $4.2$  K, which indicates that, once the phase I is established, it stays stable down to zero field.<sup>5,10</sup>

We now turn to Fig. 3 and discuss the overall picture of the magnetotransport properties in CeP. The zero-field resistivity shows a peak just above  $T_N$ , which is probably ascribed to critical scattering. Since the wave vector of the type-I antiferromagnetic structure links the hole pockets to the electron ones (located at the  $\Gamma$  and  $X$  points in the Brillouin zone, respectively), antiferromagnetic fluctuations may contribute substantially to the resistivity through inter-pocket scattering. Then, the subsequent descent is partly ascribable to quenching of those fluctuations. However, it also seems that part of the resistivity reduction can be connected with the appearance of  $\Gamma_8$  layers at the  $\alpha$  transition, since considerable decrease occurs in the temperature region where hysteresis appears and hence the  $\alpha$  transition takes place. The suppression of the resistivity at the appearance of  $\Gamma_8$  layers is more evident for the traces measured in fields; a large sharp drop occurs at the  $F(\Gamma_8)$  transition.

The  $p$ - $f$  mixing model (Ref. 14) and its expansion, the magnetic polaron model,<sup>1,15,16</sup> proposed by Kasuya *et al.* provide a possible explanation for the strong influence of  $\Gamma_8$  layers on the resistivity. The  $p$ - $f$  mixing model successfully explained the anomalous physical properties of CeSb,<sup>14</sup> in which the  $\Gamma_8$  state appears in magnetically ordered phases

despite the  $\Gamma_7$  crystal-field ground state in the paramagnetic phase. The model emphasizes the strong mixing between the  $\Gamma_8$  state of  $\text{Ce}^{3+}$  ion and the valence holes of mainly Sb  $p$  character, which has the same  $\Gamma_8$  symmetry at the  $\Gamma$  point in the Brillouin zone. Through the bonding-antibonding effect, the  $\Gamma_8$  state is stabilized, becoming the ground level in the ordered states.

An obstacle to the direct application of the  $p$ - $f$  mixing model to CeP is that the crystal-field splitting is too large to be overcome by the mixing, about  $160$  K compared with  $35$  K in CeSb. To deal with the problem, Kasuya and coworkers have recently proposed formation of magnetic polarons in CeP.<sup>1,15,16</sup> The essence of the idea is to localize holes around the  $\Gamma_8$  states and thus to enhance the hole density locally, which strengthens the  $p$ - $f$  mixing. Based on a simple free-energy model, they have claimed that, although the  $\Gamma_7$  state remains the ground level in the paramagnetic phase, the magnetic polarons, i.e., the  $\Gamma_8$  state plus localized holes, exist even at room temperature through thermal activation. Those magnetic polarons strongly scatter conduction carriers, which explains the large resistivity in CeP in a high-temperature region ( $T > \sim 80$  K). Further, the model predicts that the magnetic polarons form a lattice at a sufficiently low temperature through a first-order transition, to which the transitions  $\alpha$  and  $F(\Gamma_8)$ , or the appearance of ferromagnetic  $\Gamma_8$  layers, can be ascribed. The transition is expected to accompany a decrease in the resistivity since the magnetic polarons are no longer random scattering centers (given that their lattice is perfectly periodic). The model is attractive in that it can afford a unified picture of various anomalies seen in CeP.<sup>1,15,16</sup> However, it still lacks direct evidence for the magnetic polarons and remains to be verified by further studies.

Finally, we note that the transport behavior presented here bears resemblance to the colossal magnetoresistance (CMR) effect. Especially, our attention is led to the nonperovskite CMR compound  $\text{Tl}_2\text{Mn}_2\text{O}_7$ .<sup>17</sup> We may also cite  $\text{EuB}_6$ , which shows CMR-like transport behavior.<sup>18</sup> Both compounds are known to be a semimetal with very low-carrier density (Refs. 17 and 19) and formation of magnetic polarons has been argued.<sup>20,21</sup> Comparative studies of these materials could be helpful to elucidate mechanisms of nonperovskite CMR phenomena.

<sup>1</sup>T. Kasuya, T. Suzuki, and Y. Haga, J. Phys. Soc. Jpn. **62**, 2549 (1993).

<sup>2</sup>For a review, see, T. Suzuki *et al.*, Physica B **206&207**, 771 (1995).

<sup>3</sup>Y. S. Kwon, Y. Haga, O. Nakamura, T. Suzuki, and T. Kasuya, Physica B **171**, 324 (1991).

<sup>4</sup>Y. Haga, Y. S. Kwon, T. Suzuki, and T. Kasuya, Physica B **199&200**, 525 (1994).

<sup>5</sup>M. Kohgi, T. Osakabe, K. Kakurai, T. Suzuki, Y. Haga, and T. Kasuya, Phys. Rev. B **49**, 7068 (1994); M. Kohgi, T. Osakabe, K. Iwasa, J. M. Mignot, I. N. Goncharenko, Y. Okayama, H. Takahashi, N. Mori, Y. Haga, and T. Suzuki, J. Phys. Soc. Jpn. Suppl. B **65**, 99 (1996).

<sup>6</sup>T. Inoue, T. Kuroda, K. Sugiyama, Y. Haga, T. Suzuki, and M.

Date, J. Phys. Soc. Jpn. **64**, 572 (1995).

<sup>7</sup>T. Terashima, S. Uji, H. Aoki, J. A. A. J. Perenboom, Y. Haga, A. Uesawa, T. Suzuki, S. Hill, and J. S. Brooks, Phys. Rev. B **58**, 309 (1998).

<sup>8</sup>H. Heer, A. Furrer, W. Hälg, and O. Vogt, J. Phys. C **12**, 5207 (1979).

<sup>9</sup>K. Iwasa, M. Kohgi, Y. Haga, T. Suzuki, K. Kakurai, M. Nishi, K. Nakajima, P. Link, A. Gukasov, and J.-M. Mignot, Physica B **259-261**, 285 (1999).

<sup>10</sup>Y. Haga, Doctor of Science thesis, Tohoku University, 1994; the phase diagram determined from low-field magnetization studies and results of specific heat measurements are cited in Refs. 12 and 16, respectively.

<sup>11</sup>T. Terashima, S. Uji, H. Aoki, W. Joss, Y. Haga, A. Uesawa, and



- T. Suzuki, Phys. Rev. B **55**, 4197 (1997).
- <sup>12</sup>T. Takeuchi, K. Iizuka, K. Iwasa, M. Kohgi, Y. Haga, and T. Suzuki, J. Phys. Soc. Jpn. **67**, 2094 (1998).
- <sup>13</sup>K. Iwasa, M. Kohgi, H. Ohsumi, K. Tajima, T. Takeuchi, Y. Haga, A. Uesawa, and T. Suzuki, J. Phys. Soc. Jpn. **68**, 881 (1999).
- <sup>14</sup>H. Takahashi and T. Kasuya, J. Phys. C **18**, 2697 (1985); **18**, 2709 (1985); **18**, 2721 (1985); **18**, 2731 (1985); **18**, 2745 (1985); **18**, 2755 (1985).
- <sup>15</sup>T. Kasuya, Y. Haga, T. Suzuki, T. Osakabe, and M. Kohgi, J. Phys. Soc. Jpn. **62**, 3376 (1993).
- <sup>16</sup>T. Kasuya, J. Phys. Soc. Jpn. Suppl. B **65**, 78 (1996).
- <sup>17</sup>Y. Shimakawa, Y. Kubo, and T. Manako, Nature (London) **379**, 53 (1996).
- <sup>18</sup>C. N. Guy, S. von Molnar, J. Etourneau, and Z. Fisk, Solid State Commun. **33**, 1055 (1980).
- <sup>19</sup>R. G. Goodrich, N. Harrison, J. J. Vuillemin, A. Teklu, D. W. Hall, Z. Fisk, D. Young, and J. Sarrao, Phys. Rev. B **58**, 14 896 (1998).
- <sup>20</sup>P. Majumdar and P. Littlewood, Phys. Rev. Lett. **81**, 1314 (1998).
- <sup>21</sup>P. Nyhus, S. Yoon, M. Kauffman, S. L. Cooper, Z. Fisk, and J. Sarrao, Phys. Rev. B **56**, 2717 (1997).